Research Article

SURFACE AND INTERFACE ANALYSIS

Received: 23 June 2009 Revised: 23 December 2009 Accepted: 29 December 2009 Published online in Wiley Interscience: 19 February 2010

(www.interscience.wiley.com) DOI 10.1002/sia.3198

Inhibition effect of cerium in hybrid sol–gel films on aluminium alloy AA2024†

L. Paussa,[a]* N. C. Rosero-Navarro,[b] F. Andreatta,[a] Y. Castro,[b] A. Duran,[b] M. Aparicio[b] and L. Fedrizzi[a]

Aluminium alloys such as AA2024 are susceptible to severe corrosion attack in aggressive solutions (e.g. chlorides). Conversion coatings, like chromate, or rare earth conversion coatings are usually applied in order to improve corrosion behaviour of aluminium alloys. Methacrylate-based hybrid films deposited with sol–gel technique might be an alternative to conversion coatings. Barrier properties, paint adhesion and possibly self-healing ability are important aspects for replacement of chromate-based pre-treatments. This work evaluates the behaviour of cerium as corrosion inhibitor in methacrylate silane-based hybrid films containing SiO_2 nano-particles on AA2024. Hybrid films were deposited on aluminium alloy AA2024 by means of dip-coating technique. Two different types of coating were applied: a non-inhibited film consisting of two layers (non-inhibited system) and a similar film doped with cerium nitrate in an intermediate layer (inhibited system). The film thickness was 5 μm for the non-inhibited system and 8 μm for the inhibited system. Film morphology and composition were investigated by means of GDOES (glow discharge optical emission spectroscopy). Moreover, GDOES qualitative composition profiles were recorded in order to investigate Ce content in the hybrid films as a function of immersion time in 0.05 M NaCl solution. The electrochemical behaviour of the hybrid films was studied in the same electrolyte by means of EIS technique (electrochemical impedance spectroscopy). Electrochemical measurements provide evidence that the inhibited system containing cerium displays recovery of electrochemical properties. This behaviour is not observed for the non-inhibited coating. GDOES measurements provide evidence that the behaviour of inhibited system can be related to migration of Ce species to the substrate/coating interface.

Keywords: hybrid coatings; rare earth elements; sol–gel; Cr-free pre-treatment; aluminium

Introduction

In order to obtain corrosion protective systems alternative to Cr-based coatings, different types of coatings have been recently developed for various metal substrates. In particular, there is a strong demand for Cr-free coatings for corrosion protection of aluminium alloys such as AA2024. At present, chromate conversion coating represents the state of the art for industrial applications.[1,2] Unfortunately, coatings containing chromates are dangerous and are not environment-friendly.[3–5]

In this work, alternative coatings produced via sol–gel were developed in order to replace chromate-based systems. Thin films or thick films are obtained by means of sol–gel method controlling solution concentration, dip number or withdrawal rate.[1] This technique enables to deposit at low temperature – typically below 200 °C – inorganic or organic–inorganic coatings.[6–9] Hybrid coatings link together properties of organic and inorganic materials. Organic fractions enable to obtain a more ductile system with less stress tensions than the traditional inorganic ones. Moreover, it is possible to produce a thicker coating without formation of cracks.[10] In order to increase density and mechanical properties of hybrid films, silica nano-particles can be added to the system.[11]

This work investigates hybrid inorganic–organic coatings reinforced with silica nano-particles. In order to study cerium inhibition ability, doped systems were obtained adding cerium nitrate into the starting solution. Dip-coating technique was employed to deposit hybrid systems.

Impedance measurements were carried out on two types of sample (non-inhibited without cerium and inhibited with cerium). Qualitative glow discharge optical emission spectroscopy (GDOES) profiles were detected in order to study cerium diffusion and inhibition.

Experimental Procedure

The metal AA2024-T3 was employed as substrate. Prior to deposition, the aluminium alloy underwent surface preparation including alkaline cleaning (Metaclean T2001 – Chemie Vertrieb Hannover GmbH & Co KG), alkaline etching (Turco Liquid Aluminetch Nr.2 – Turco Chemie GmbH) and acid etching (Turco Liquid Smutgo NC – Turco Chemie GmbH). The procedure described above enables to remove the oxide layer present on the as-received material and to partially remove the intermetallic particles from the alloy surface.

* *Correspondence to: L. Paussa, Department of Chemical Science and Technology, University of Udine, Via del Cotonificio, 108, 33100, Udine, Italy. E-mail: luca.paussa@uniud.it*

† *Paper published as part of the Aluminium Surface Science & Technology 2009 special issue.*

a *Department of Chemical Science and Technology, University of Udine, Via del Cotonificio 108, 33100, Udine, Italy*

b *Instituto de Cerámica y Vidrio (CSIC), Campus de Cantoblanco, 28049, Madrid, Spain*

The procedure for the preparation of the sol solution is similar to that described in another publication and will not be discussed in detail in this paper.[12] Starting precursors were tetraethoxysilane (TEOS, ABCR 98%), methacryloxypropyl trimethoxysilane (MPS, ABCR, 98%) and colloidal SiO_2 (Ludox-4S, Aldrich, aqueous suspension 40 wt%, particle size 20 nm, pH 9). The SiO_2 nano-particles were added to the precursor in order to improve the cross-linking between the inorganic groups of the precursor.[12] Indeed, hydrolysed alkoxides can bond with the silica surface forming siloxane bond or hydrogen bond promoting the formation of a higher cross-linked structure.[13] Moreover, the addition of SiO_2 nano-particles increases density and mechanical properties of the sol–gel coatings.[12] The addition of dense silica nano-particles (2.25 g/cm^3) to a lower density matrix (<2 g/cm^3) will result in an increment of the total density. This improves scratch resistance and hardness of sol–gel coatings loaded with nano-particles.[14]

Etylenglicol dimethacrylate (EGDMA, Aldrich 98%) and glycidyl methacrylate (GMA, Aldrich, 98%) were used as organic monomers. Initiation of the organic polymerisation was 2,2′-azobis (isobutyronitrile) (AIBN, Aldrich, 98%). Cerium nitrate ($Ce(NO_3)_3$ $6H_2O$, Aldrich 99%) was employed as source of cerium ions. The sol solution was obtained controlling separately inorganic and organic polymerisations. After hydrolysis of alkoxide groups and initiation of inorganic polycondensation, organic polymerisation was promoted adding the initiator of the reaction (AIBN) in a relation of 0.01 moles per mol of C=C groups present in the solution. Cerium doped sol was obtained adding the cerium salt into the solution with a molar ratio Ce : Si of 5 : 95 at the end of the synthesis. Cerium doped and undoped sols were used to produce corrosion protection systems for AA2024. The deposition of this protection system was carried out by means of dip-coating technique with a withdrawal rate of 20 cm/min. In order to promote polymerisation and to increase density of the structure, samples were subjected to a thermal treatment at 60 °C for 4 h followed by heating at 120 °C for 2 h. Two types of samples were produced. Non-inhibited type coatings consisted of two layers deposited with sol without cerium. Inhibited type coatings were composed of three layers. The intermediate layer is doped with cerium, whereas the other layers do not contain cerium. The coating thickness was evaluated by profilometry (Talystep, UK) and it was respectively 5 μm for the non-inhibited and 8 μm for the inhibited samples. Although coating thickness is different for the two systems considered in this work, it is interesting to compare the electrochemical behaviour of the inhibited system with the non-inhibited one in order to evaluate the effectiveness of cerium. Moreover, it should be considered that barrier properties are mainly determined by the layer without inhibitor, whereas the layer containing cerium is porous and does not act as a barrier.

Corrosion resistances and inhibition ability were investigated by means of EIS(electrochemical impedance spectroscopy). This technique enables the study of coating properties under free immersion without promoting accelerated damage of the system, in contrast to others like potentiodynamic polarisation. Electrochemical tests were carried out in an aqueous solution containing 0.05 M NaCl. The area exposed (working electrode area) to the electrolyte was 14.8 cm^2. Impedance measurements were recorded using a Pt counter electrode and Ag/AgCl reference electrode. In order to reach a steady-state condition, the impedance measurements were carried out after 15 min free immersion in the electrolyte. Impedance data were recorded at open circuit potential with an a.c. voltage amplitude of 10 mV and a frequency range from 10 mHz to 100 kHz. All impedance spectra were fitted by means of Zview Software.

In order to assess diffusion and inhibition of Ce^{3+} species in the inhibited coatings, qualitative GDOES composition profiles were carried out with a Jobin Yvon GD Profiler. Qualitative composition profiles (intensity *versus* erosion time) were acquired at different immersion times in 0.05 M NaCl aqueous solution. Cerium diffusion to the substrate can be studied integrating the area below the cerium signal. This area is representative of the amount of cerium diffused towards the interface. The integration was done between the coating/substrate interface and a point corresponding to an erosion time of 10 s lower than that associated with the interface. In order to better study possible diffusion, the intensity (V) of the recorder GDOES signal of cerium has been evaluated for different immersion times at a sputtering time of 115 s. This corresponds to a region in the proximity of the coating/metal interface. This approach enables us to study the Ce^{3+} diffusion to the metallic substrate by evaluating intensity and shape of cerium signal in the GDOES qualitative profiles.

Results

Electrochemical impedance measurements were performed on non-inhibited and inhibited samples. The Nyquist plot is reported because it is a helpful tool to compare the electrochemical behaviour for the two hybrid systems investigated. In the impedance spectra acquired on electrochemical systems, the contribution related to the faradic reactions can be often identified at low frequency. This enables us to obtain information about the corrosion rate of the substrate by evaluating the diameter defined by the semi-circle at low frequency. Figure 1 reports the Nyquist plot for the inhibited and the non-inhibited systems in 0.05 M NaCl solution as a function of immersion time. After 30 min immersion (Fig. 1(a)), the semi-circle relative to the electrochemical contribution provided by the hybrid coatings can be identified at high frequency. It can be seen that the initial barrier properties evidenced by the inhibited system are better than those for the non-inhibited one. This might be related to the different thickness of the two types of coatings. However, it can be expected that the contribution to the barrier properties of the layer containing cerium is very limited due to the high porosity of this layer. It might be considered that it is difficult to compare systems with different thicknesses. However, it was necessary to produce an inhibited multilayer system because it was demonstrated in our previous work[15] that it was very difficult to introduce cerium species in a sol–gel monolayer with good barrier properties. Furthermore, it was shown that the non-inhibited monolayer system evidenced a slow reduction of barrier properties as a function of immersion time and that incorporation of cerium ions in a sol–gel monolayer led to the formation of an open structure with high porosity.[15] Therefore, the high porosity of the inhibited monolayer systems is the major cause for coating degradation because it favours the formation of conductive paths in the coating. Consequently, the barrier properties of a non-inhibited system consisting of two layers are expected to be in the same range of those of a similar system with an additional intermediate layer containing cerium.

The trend of Nyquist plots at low frequency in Fig. 1(a) provides information on faradic reactions at the metal substrate. The behaviour of the two systems is slightly different after 30 min of immersion at low frequency. The slope of the curve relative to

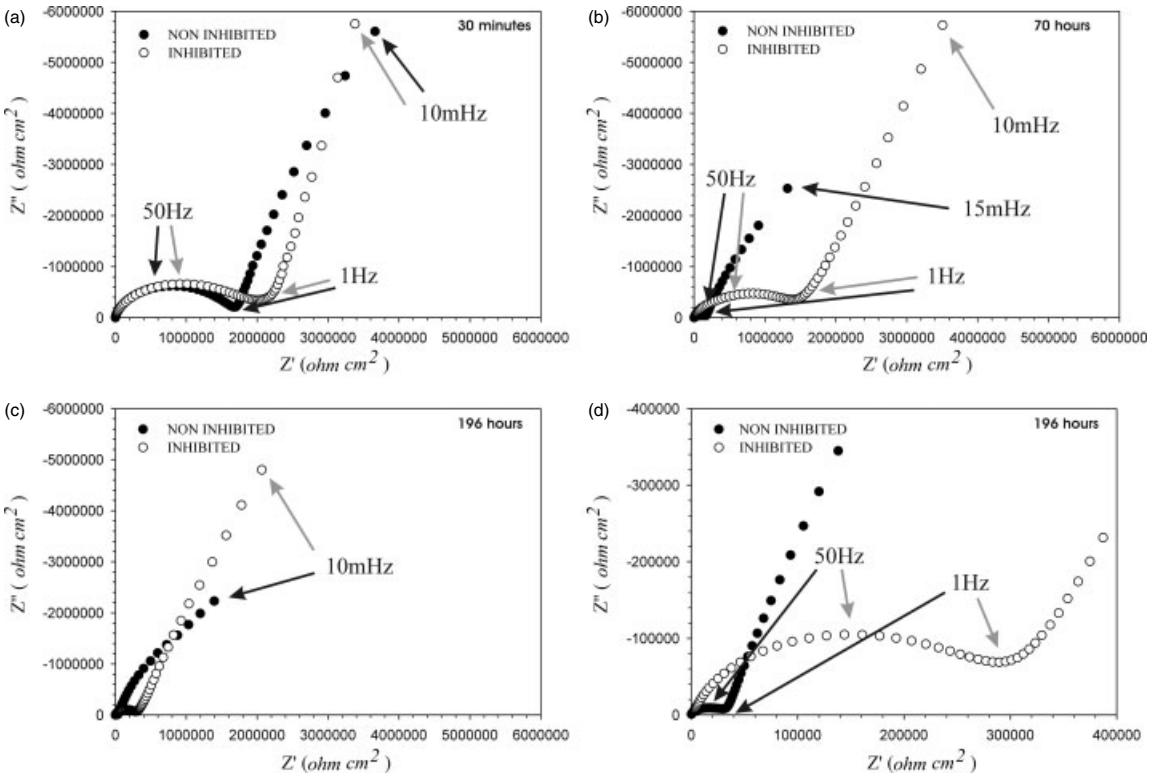

Figure 1. Nyquist plots of electrochemical impedance recorded after 30 min (a), 70 h (b) and 196 h (c) for inhibited and non-inhibited hybrid coatings on AA2024-T3. A detail of the Nyquist plot after 196 h is also reported in (d).

the inhibited system seems slightly higher at low frequency than that of the non-inhibited system. Thus, it can be expected that the corrosion rate for the inhibited system is lower than for the non-inhibited one.

After 70 and 196 h of immersion (Fig. 1(b) and (c)), the two systems provide evidence for a fast degradation of barrier property. However, this degradation occurs with slower rate for the non-inhibited system with respect to the inhibited one. This is evident in the Nyquist plot after 70 h. However, both systems provide a very limited protection after 196 h (Fig. 1(d)) which is about ten times lower than the initial value immediately after immersion.

Although barrier properties are limited, the two systems considered in Fig. 1(b) and (c) provide evidence for different behaviour at low frequency. Indeed, the slope of the plots at low frequency is higher for the inhibited system than for the non-inhibited one suggesting that the former system is characterised by a lower corrosion rate than the latter.

Since the Nyquist plots in the figure indicate an inhibition effect due to the incorporation of cerium in the hybrid system, impedance data were fitted in order to further investigate the corrosion behaviour of the two hybrid systems considered in this work. Figure 2 shows the electrochemical equivalent circuit employed to fit impedance data. In this circuit, the constant phase element (CPE) was used instead of an ideal capacitor. This was necessary in order to explain the deviation from the ideal behaviour of a real component. A CPE is often used to compensate for non-homogeneity of the system.

The impedance of the CPE is defined by the following equation:[16]

$$Z_{CPE} = \frac{1}{T(i\omega)^P} \quad (1)$$

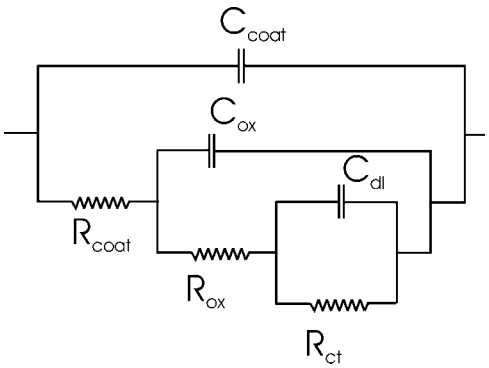

Figure 2. Equivalent circuit employed for fitting electrochemical impedance data.

where T is a pseudo-capacitance, i is the imaginary coefficient, ω the angular frequency and P describes the deviation from the ideal behaviour. If P equals 1, the previous equation corresponds to a pure capacitor.

In Fig. 2, R_{coat} is the resistance of the sol–gel coating, R_{ox} is the resistance associated with the thin aluminium oxide layer and R_{ct} is the charge transfer resistance describing corrosion reactions on the metallic substrate. The real part of impedance is determined mainly by these resistances. These resistances provide information about physical barrier of the coating, defects and possible inhibition due to species contained in the system. C_{coat} is the pseudo-capacitance associated with the insulating ability of the coating, C_{ox} is the pseudo-capacitance of the aluminium oxide layer and C_{dl} is the double-layer pseudo-capacitance related to

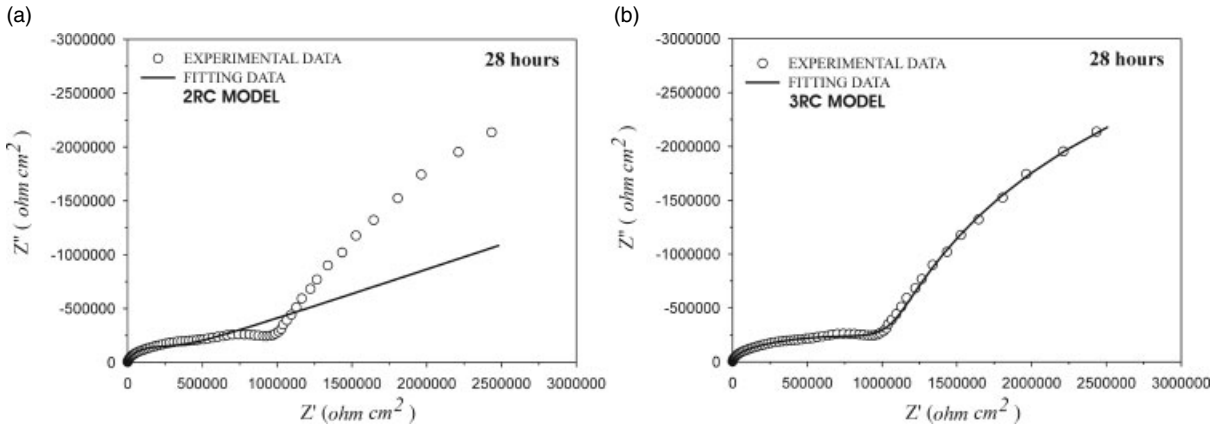

Figure 3. Fit results of electrochemical impedance data recorded for non-inhibited hybrid coating employing a two time constants (a) and a three time constants equivalent circuit (b).

the adsorbed anions layer on the metal surface and to diffuse the mobile cations layer in the electrolyte solution.

Figure 3 shows fit results obtained by employing a two times constant equivalent circuit and the equivalent circuit described in Fig. 2. The two times constant equivalent circuit was initially used for fitting impedance data. This was based on the assumption that the electrochemical behaviour of a system with good barrier properties can be described with two time constants, one associated with the coating and the other with the metal substrate. As can be seen in Fig. 3(a), the fit result was not satisfactory employing the two time constants. In particular, the fit results exhibit a significant error at low frequency preventing a correct evaluation of the effect of cerium on corrosion behaviour. Therefore, it was necessary to employ the equivalent circuit shown in Fig. 2 to fit the experimental data. Figure 3(b) shows fit results that are more accurate and provide reliable information about the electrochemical behaviour of the system investigated. In particular, experimental data are fitted with very good accuracy at low frequency.

Figure 4(a)–(c) shows the trend of R_{coat}, R_{ox} and R_{ct} as a function of immersion time for non-inhibited and inhibited samples obtained employing the equivalent circuit shown in Fig. 2. In Fig. 4(a) fast reduction of R_{coat} is visible for non-inhibited and inhibited coatings. This behaviour is connected to fast water absorption due to the rather high intrinsic porosity of hybrid coatings considered in this work.[12] Water uptake leads to an increase of film conductivity that causes the R_{coat} reduction. It is possible to note that the starting values of R_{coat} (immediately after immersion in the electrolyte solution) for the non-inhibited and inhibited systems are different. This is most likely correlated to the different thickness of non-inhibited and inhibited structures. The coating resistance (barrier properties) is higher for thick film than for thinner ones. Indeed, the inhibited coating is 8 µm thick while the non-inhibited system is 5 µm. However, it should be noted that the trend of R_{coat} is very similar for the two coatings.

The coating porosity is deliberately kept high to promote Ce^{3+} species diffusion outwards the intermediate layer of the inhibited system. The inhibited system is developed as a primer coating. Therefore, in order to evaluate the corrosion resistance related to Ce^{3+}, the inhibited system should be characterised after application of a top coat. These aspects will be discussed in more detail in a future paper. However, a porous coating is desired to promote active migration of cerium to the metallic substrate. This migration might promote inhibition improving the corrosion resistance. Therefore, possible inhibition due to cerium might be recognised by comparing the behaviour of the coating doped with the inhibitor (inhibited) and a similar coating without inhibitor (non-inhibited). As seen above, impedance data were initially fitted employing two RC meshes, the first associated with the hybrid coating and the second with the faradic reactions. The quality of the fit employing two RC meshes was not good. In order to improve the fit results, the equivalent circuit was implemented with a third RC mesh (Fig. 2) because a new time constant was visible at medium frequencies. The third time constant is not always clearly distinguishable in impedance spectra because it overlaps with the contribution of the other RC meshes. The new mesh is related to resistance (R_{ox}) and capacitance (C_{ox}) of an intermediate oxide layer associated with the passivity of the metallic substrate.

Figure 4(b) shows R_{ox} values of inhibited and non-inhibited samples. It can be seen that R_{ox} is higher for the inhibited coating than for the non-inhibited one. The different R_{ox} trends could be explained considering the cerium effect. As considered above, Ce^{3+} ions diffusion is favoured in a porous coating. Cerium precipitation in the form of hydroxide or oxide is likely to occur on the metallic substrate due to *red-ox* reactions activated by local variations of parameters like pH or oxygen and chloride concentration. These might activate cathodic inhibition according to mechanisms proposed in the literature.[17] These mechanisms are associated with cathodic reactions on the metallic surface that locally can lead to a pH variation. Therefore, the preferential sites of Ce^{3+} precipitation on the metallic substrate are cathodic areas.[18,19] In AA2024, cathodic areas are mainly due to precipitation of intermetallic phases in the matrix. Cerium precipitation is most likely to occur increasing the driving force. The existence of a better barrier (higher R_{ox}) for the inhibited system than for the non-inhibited one is attributed to precipitation of cerium at the coating/substrate interface promoting a stable oxide layer.

Figure 4(c) shows R_{ct} trends for inhibited and non-inhibited systems as a function of immersion time. This electrical component is directly connected to *red-ox* processes on the metallic substrate and it is inversely proportional to the corrosion rate. R_{ct} of the non-inhibited system continuously decreases as a function of immersion time. In contrast, R_{ct} of the inhibited coating exhibits an initial increase during the 100 h in the electrolyte followed by a

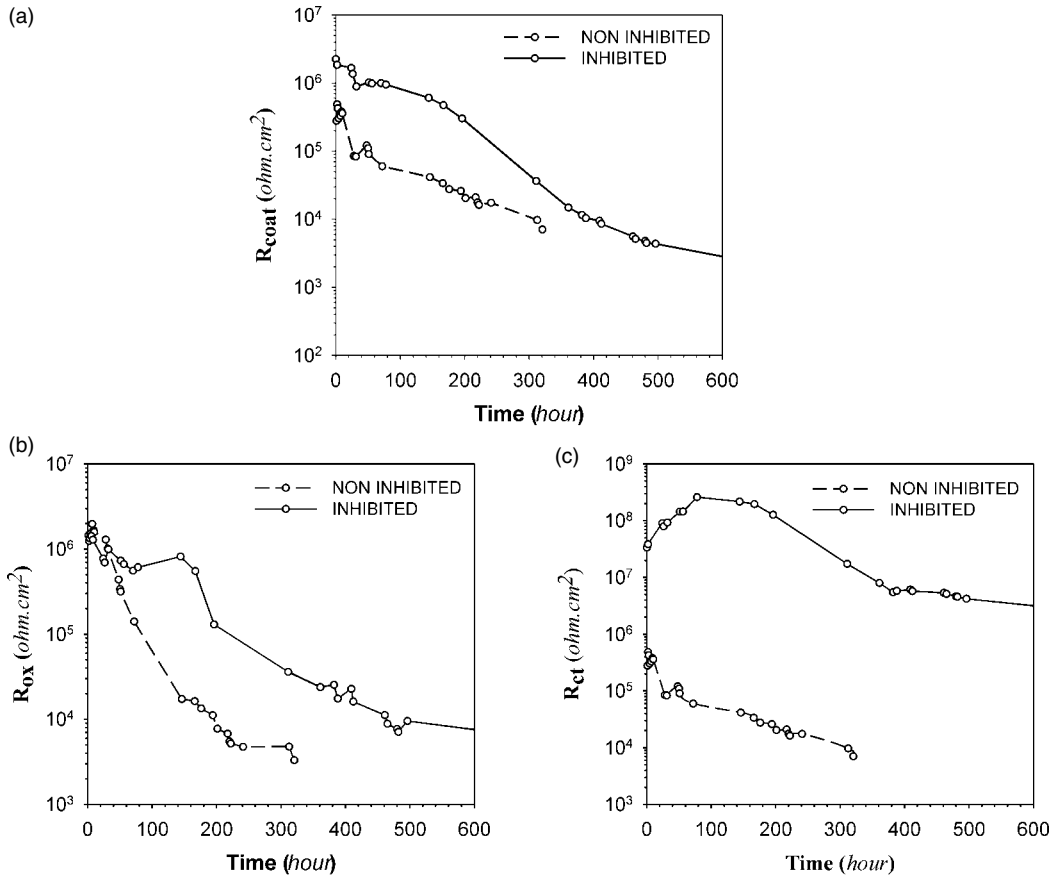

Figure 4. R_{coat} (a), R_{ox} (b) and R_{ct} (c) as a function of immersion time in 0.05 M NaCl solution.

progressive decrease until a stable value is reached after 350 h of immersion. The first R_{ct} increase for this system is probably due to the precipitation of Ce^{3+}, which promotes the formation of a more uniform oxide layer on the substrate reducing active areas. This is associated with a lower corrosion rate of the metal substrate in the inhibited system than in the non-inhibited one. The following decrease of R_{ct} of the inhibited coating is probably due to the gradual reduction of free Ce^{3+} available in the coating. Indeed, other areas of the substrate might become active increasing immersion time due to progressive loss of adhesion between coating and substrate. Although degradation of the passive oxide layer is visible for the inhibited system, R_{ct} values observed for this sample remain three orders of magnitude higher than the non-inhibited one.

In order to verify results obtained by means of electrochemical impedance technique, GDOES measurements were carried out on the inhibited coating to evaluate cerium mobility in this system.

The diffusion action of aqueous solution combined with the chloride content has led to the evaluation of the cerium behaviour. By means of this experimental approach, it has been possible to determine and to verify the protective mechanism of cerium doped hybrid coatings explained in the electrochemical section.

Figure 5 shows the qualitative composition profiles of the inhibited system before immersion, and after 3 and 56 h of immersion in a 0.05 M NaCl solution. These profiles were recorded in different areas of the sample surface. However, coating thickness and surface roughness were the same for the test areas. Moreover, the area analysed with the GDOES was 12 mm^2. This is a relatively large area and can be considered reliable for the evaluation of cerium behaviour. The GDOES qualitative profiles shown in Fig. 5 display the carbon signal associated with hybrid coating, the aluminium signal relative to the metallic substrate and cerium signal (with a multiplicative factor of 1000) due to a presence of cerium in the intermediate doped layer.

In Fig. 5, shape and intensity of carbon signal are similar for the three different immersion times. This confirms that erosion rate is similar for the three areas characterised and suggests that the measurement is not significantly affected by water uptake.

The cerium signal evidences the existence of the inhibitor in the intermediate layer. Before immersion (Fig. 5(a)), the interface between the outer layer (without cerium) and the intermediate layer (cerium doped) is identified at 40 s of erosion. The slope of the cerium signal at this interface progressively decreases after 3 and 56 h (Fig. 5(b) and (c)) of immersion. In particular, this is evident after 56 h of immersion. For this immersion time, it is not possible to clearly identify the interface between the outer layer and the cerium doped layer as the transition is rather broad. This observation indicates that part of cerium in the intermediate layer diffuses to the electrolyte. Therefore, the total amount of cerium in the inhibited system after 56 h of immersion is lower than the amount in the system immediately after immersion. The interface between the metal substrate and coating can be arbitrarily located at the intersection between carbon and aluminium signals. This is located at about 120 s of erosion time for the three different immersion times. An increase of the signal intensity of cerium is detected at the interface region between coating and substrate for 3 and 56 h of immersion time relative to the signal before immersion. As an indication, the intensity of the recorded GDOES

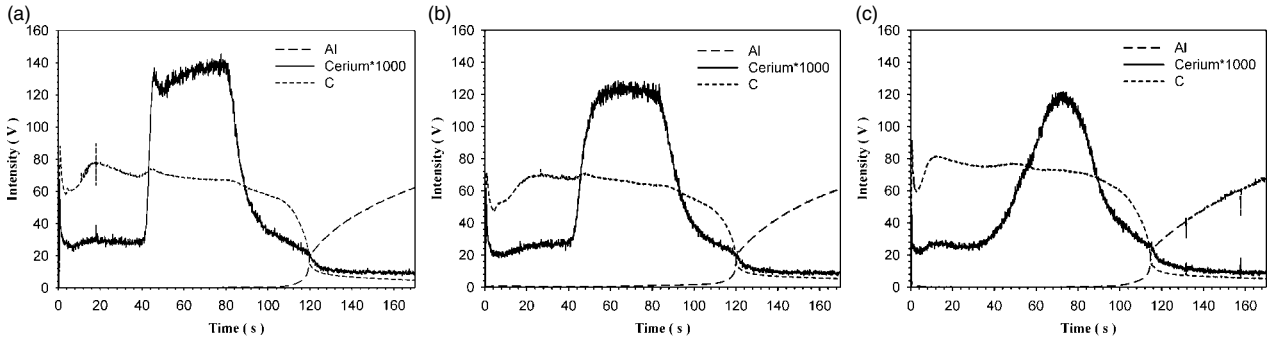

Figure 5. Qualitative GDOES profiles for inhibited system (a) before immersion, (b) after 3 h and (c) after 56 h of immersion in 0.05 M NaCl solution.

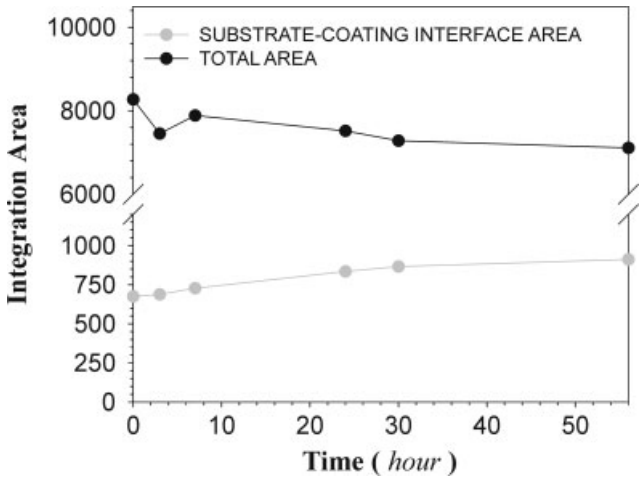

Figure 6. Integration area below cerium signal as a function of immersion time.

signal of cerium is 24 V immediately after immersion, 25 V after 3 h of immersion and 28 V after 56 h of immersion. This corresponds to an intensity increase of 14% after 56 h in solution with respect to the same signal immediately after immersion. This is further evidenced by a gradual increase of the slope of the curve relative to cerium. The increase of the slope is associated with accumulation of cerium at the substrate. This is most likely due to precipitation of a cerium hydroxide or oxide. The trend of cerium signal is in line with the results of electrochemical characterisation by means of impedance spectroscopy, as evidenced by the trend of R_{ox} and R_{ct} for similar immersion times. Cerium diffusion to the substrate can be further studied by integrating the area below the cerium signal in Fig. 5. This area is representative of the amount of cerium diffused at the interface. The integration was done between the coating/substrate interface and a point corresponding to an erosion time of 10 s lower than that associated with the interface. This approach enables to obtain qualitative information about the amount of cerium diffused at the interface.

Figure 6 shows the trend of the amount of cerium calculated as described above as a function of the immersion time (substrate/coating interface area). This area progressively increases with immersion time confirming the qualitative analysis of GDOES profiles and electrochemical impedance measurements. In addition, the total area below the curve relative to cerium signal is also represented in Fig. 6. The total area has been calculated over the entire coating thickness (between the substrate/coating interface and the coating surface). The estimation of the total area provides information about cerium present in the coating. As it can be seen in Fig. 6, the total area decreases as a function of immersion time. This result is due to diffusion of Ce^{3+} species in the direction of bulk solution.

Although this trend indicates that there is a marked depletion of cerium in the inhibited coating, a fraction of Ce^{3+} ions moves towards the metal/coating interface. This aspect is very important in the view of corrosion protection because the mechanism related to cerium could take place at the metal coating interface with an inhibition effect on corrosion reactions. It is also possible that cerium diffusion to the substrate is promoted by water flow to the interface related to water uptake. As discussed above, this behaviour should also be investigated for a system consisting of inhibited film and top coat. In this case, diffusion of Ce^{3+} ions towards bulk solution could be limited by the top coat, and the amount of cerium species available for the protection of the metallic substrate is likely to be higher than for the inhibited system without top coat.

Conclusions

Sol–gel hybrid inorganic–organic coatings applied on AA2024 have been investigated by means of EIS. Qualitative GDOES profiles have been carried out on inhibited samples to evaluate the inhibition effect of cerium.

Corrosion properties of inhibited system containing cerium are better than those of non-inhibited ones. Impedance investigations indicate that the aluminium oxide layer on the substrate is modified by cerium precipitation. The mobility of Ce^{3+} ions towards the substrate is favoured by the porosity of the hybrid films.

GDOES measurements show a reduction of total amount of cerium present in the inhibited system as a function of immersion time. A fraction of cerium moves to bulk solution, while significant cerium diffusion is evidenced in the direction of the metal substrate. This is associated with a marked improvement of corrosion resistance of the inhibited system containing cerium relative to the non-inhibited coating.

Acknowledgements

This paper and the work it concerns were generated in the context of the MULTIPROTECT project, funded by the European Community as contract No NMP3-CT-2005-011783 under the Sixth Framework Programme for Research and Technological Development. Friuli Innovazione is kindly acknowledged for the technical support provided in this work.

SURFACE and INTERFACE ANALYSIS

References

[1] T. L. Metroke, R. L. Parkhill, E. T. Knobbe, *Prog. Org. Coat.* **2001**, *41*, 233.
[2] P. Campestrini, E. P. M. van Westing, A. Hovestad, J. H. W. de Wit, *Electrochim. Acta* **2002**, *47*, 1098.
[3] M. Bethencourt, F. J. Botana, J. J. Calvino, M. Marcos, M. A. Rodriguez-Chacon, *Corros. Sci.* **1998**, *11*, 1803.
[4] J. H. Osborn, *Prog. Org. Coat.* **2001**, *41*, 280.
[5] U.S. Public Health Service, Report no. STSDR/TP-88/10 July, **1989**.
[6] M. Guglielmi, *J. Sol-Gel Sci. Technol.* **1997**, *8*, 443.
[7] R. L. Ballard, J. P. Williams, J. M. Nius, B. R. Kiland, M. D. Soucek, *Eur. Polym. J.* **2001**, *37*, 381.
[8] A. Conde, A. Duran, J. J. de Damborenea, *Prog. Org. Coat.* **2003**, *46*, 288.
[9] W. J. V. Ooij, D. Zhu, V. Palanivel, J. A. Lamar, M. Stacy, *Silicon Chem.* **2006**, *3*, 11.
[10] S. Pellice, P. Galliano, Y. Castro, A. Duran, *J. Sol-Gel Sci. Technol.* **2003**, *28*, 81.
[11] F. Mammari, E. Le Bouhis, L. Rozesa, C. Sanchez, *L. Mater. Chem.* **2005**, *15*, 3787.
[12] N. C. Rosero-Navarro, S. A. Pellice, Y. Castro, M. Aparicio, A. Duran, *Surf. Coat. Technol.* **2009**, *203*, 1897.
[13] M. W. Daniels, L. Francis, *J. Colloid Interface Sci.* **1998**, *205*, 191.
[14] S. Pellice, P. Galliano, Y. Castro, A. Duran, *J. Sol-Gel Sci. Techol.* **2003**, *28*, 81.
[15] N. C. Rosero-Navarro, S. A. Pellice, A. Duran, M. Aparicio, *Corros. Sci.* **2008**, *50*, 1283.
[16] R. Cottis, S. Turgoose, B. C. Syrett, in *Electrochemical Impedance and Noise*, Nace International: Houston, **1999**.
[17] S. A. Hayes, Pu. Yu, T. J. O'Keefe, M. J. O'Keefe, J. O. Stoffer, *J. Electrochem. Soc.* **2002**, *12*, C623.
[18] B. F. Rivera, B. Y. Johnson, M. J. O'Keefe, W. G. Fahrenholtz, *Surf. Coat. Technol.* **2004**, *176*, 349.
[19] W. Pinc, S. Geng, M. O'Keere, W. Fahrenholtz, T. O'Keefe, *Appl. Surf. Sci.* **2009**, *255*, 4061.

